Memory Effect Manifested by a Boson Peak in Metallic Glass

P. Luo, Y. Z. Li, H. Y. Bai, P. Wen, and W. H. Wang

Phys. Rev. Lett. **116**, 175901 — Published 27 April 2016

DOI: 10.1103/PhysRevLett.116.175901

Memory effect manifested by boson peak in metallic glass

P. Luo, Y. Z. Li, H. Y. Bai, P. Wen* and W. H. Wang**

Institute of Physics, Chinese Academy of Sciences, Beijing 100190, People's Republic of China

Abstract

We explore the correlation between boson peak and structural relaxation in a typical metallic glass. Consistent with enthalpy recovery, boson peak shows memory effect in an aging-and-scan procedure. Single-step isothermal aging produces monotonic decrease of enthalpy and boson peak intensity; for double-step isothermal aging, both enthalpy and boson peak intensity experience coincidently an incipient increase to a maximum and a subsequent decrease toward the equilibrium state. Our results indicate a direct link between slow structural relaxation and fast boson peak dynamics, which presents a profound understanding of the two dynamic behaviors in glass.

*Corresponding author: pwen@iphy.ac.cn

** Corresponding author: whw@iphy.ac.cn

Metallic glasses own distinctive performances in mechanics and magnetics with respect to their crystalline counterparts. With a simple atomic packing, metallic glass offers an effective model system for the study of some controversial issues in glass science [1]. Due to its nonequilibrium nature, glass is continually relaxing toward a metastable equilibrium state, i.e., physical aging [2]. It is fraught with difficulty for modeling of glass aging and understanding its basic mechanisms due to the complex dynamics [3-10]. One peculiar phenomenon in glass aging is the memory effect, viz., during the relaxation toward its equilibrium state, a previously aged glass often shows a temporary neglect of its future (the equilibrium state) and a memory of its past, revealing history-dependent behaviors [11-15]. Memory effect is another manifestation of structural relaxation and ensures the proper description of the relaxation dynamics, thus, procures a deeper understanding of the complex glassy-state dynamics [2, 15].

Glass puzzles us not only with the localized complex atomic rearrangement arising from its nonequilibrium nature, but also with the peculiar low-frequency (terra Hertz region) enhancement of vibrational density of states as compared with the Debye square-frequency law. This excess contribution to the vibrational spectrum is called boson peak [16], and can be reflected in heat capacity C_p by a maximum over the Debye T^3 law in the temperature (T) dependence of C_p/T^3 at 5~30 K [17]. Despite the controversy, quasilocalized transverse vibrational modes associated with defective soft local structures are generally accepted as the origin of boson peak [18-20]. A number of models have been proposed for further atomistic description of the structural origin of the anomalous low-frequency excited states, for example, soft anharmonic potentials [21-23], a transition from a minima-dominated to a saddle-dominated phase [24] or strongly anharmonic transitions between local minima of the energy landscape [25], randomly fluctuating density [26] and/or elastic constants [27], low dimensional atomic chains [28], interstitialcylike “defects” [29], independent localized harmonic model involved in Einstein-type vibrations [30], and smeared out van Hove singularities [31, 32]. Regardless of their specific assumptions and interpretations, these models are commonly related to the heterogeneous nature of

glass with spatially distributed distinct subensembles contributing an excess vibrational density of states.

Some tentative efforts have been made to explore the relationship between the structural relaxation and boson peak behavior by numerical simulations. For example, based on the potential energy landscape (PEL) [33], it was found that the boson peak intensity is positively correlated with the energy of inherent structure (local minima of PEL) [24]. The simulation showed that an observed negative correlation between the fragility of the glass-forming liquid and the boson peak intensity suggested a possible link between the structural relaxation and the boson peak dynamics [18]. Whereas a compelling positive correlation between the slow structural relaxation and the fast boson peak dynamics has not been investigated experimentally in glassy state, which is of paramount importance in discriminating between these theoretical models.

In this letter, we trace the evolution of the boson heat capacity peak with the structural relaxation manifested by the relative enthalpy change. Upon single-step isothermal aging at a constant temperature, both enthalpy and boson peak intensity show a monotonic decrease toward the metastable equilibrium state. When the sample was firstly aged at a certain temperature and then stepped up to a higher one, an obvious nonmonotonic behavior emerges not only in enthalpy but also, intriguingly, in boson peak intensity, i.e., the memory effect is revealed. The memory effect manifested by boson peak behavior indicates clearly a direct link between the slow structural relaxation and the fast boson peak dynamics and brings a new perspective to the memory effect and the dynamics in glass.

The $Zr_{50}Cu_{40}Al_{10}$ bulk metallic glass (BMG) was prepared by suck-casting from master alloy ingots to a copper mold cooled by water in an arc furnace. The amorphous nature was examined by X-ray diffraction. Calorimetric measurements and isothermal aging of the samples were performed within a Perkin-Elmer differential scanning calorimetry (DSC 8000) in high-purity standard aluminum crucibles under a constant flow of high-purity argon gas (20 ml/min). The glass transition temperature, T_g and crystallization temperature, T_x at a heating rate of 40 K/min are 703 K and 795 K, respectively. Low temperature heat capacity C_p was

measured with a Quantum Design physical property measurement system, in the temperature range of 2~40 K. The samples, 2 mm in diameter with a mass of around 20 mg, were carefully polished for good thermal contact and placed on top of a sapphire block of known heat capacity with a thermal grease to ensure good thermal contact. Prior to the sample measurement, we measured the heat capacity of an empty sapphire crystal with the applied grease for baseline correction. For enthalpy relaxation experiments, BMG disks with a mass of around 150 mg were cut from a rod with 5 mm in diameter and carefully polished for good thermal contact.

We compared the time evolution of enthalpy recovery and boson heat capacity peak in samples during single- and double-step isothermal aging. The aging protocols are schematically illustrated in Fig. S1 in the Supplemental Materials [34]. For the single-step aging (Fig. S1(a) [34]), the BMG sample was firstly heated up from room temperature (RT) to 748 K (in supercooled liquid temperature region) at 40 K/min and then cooled down to RT at 80 K/min to erase the thermal history from the preparation. A following calorimetric scan at 40 K/min was carried out to determine a reference heat flow curve of the sample previously cooled from 748 K at 80 K/min. The sample was then cooled from 748 K to the aging temperature T_a= 688 K at 80 K/min and held for an aging time t_a, and then was cooled down to RT at 80 K/min. Finally, a calorimetric scan at 40 K/min was carried out to measure the heat flow of the aged sample. The double-step aging (Fig. S1(b) [34]) involved a pre-aging step at temperature T_0 for time t_0, after which the temperature was stepped up to T_a= 688 K at 80 K/min. The amorphous nature of the aged samples was ensured by measuring the enthalpy of crystallization and XRD.

Figure 1 plots the enthalpy recovery heat flow curves after single- and double-step isothermal aging. During the single-step aging [Fig.1 (a)], as t_a increases, the endothermal peak becomes enhanced and broadens, showing a typical structural relaxation of glass [2]. While for the double-step aging [Fig.1 (b)], as the sample was pre-aged at a lower temperature before the second step aging, the endothermal peak firstly decreases and then increases with t_a. The relative enthalpy change ΔH can be calculated by subtracting the temperature integral of the heat flow curve of the aged

state from that of the reference state. As shown in the inset of Fig. 1(a), during the single-step aging (see the solid red line) the relative enthalpy change ΔH as a function of t_a decreases monotonically toward the equilibrium value [shown by curve A in Fig. 3 (a)]; while the double-step aging [see the dash green line in the inset of Fig. 1(a)] produces a nonmonotonic evolution of the ΔH with t_a [curve C in Fig. 3 (a)].

The aging protocol of the samples for low-T heat capacity measurements was similar to, yet slightly different from what for enthalpy measurements (Fig. S1 [34]). The sample was heated up from RT to 748 K at 40 K/min and then immediately cooled down to the aging temperature (T_a for single-step aging or T_0 for double-step aging) at 80 K/min, without the second and last up-scans to measure the heat flow. Figure 2 plots the measured low-T heat capacity of aged samples as $(C_p\text{-}C_p^{\text{cryst}})/T^3$ vs. T, making visible the boson peak contribution. C_p^{cryst} represents the measured low-T heat capacity of the crystalline $Zr_{50}Cu_{40}Al_{10}$ sample which was obtained by heating the glassy sample to 823 K and held for 3 min for full crystallization. C_p^{cryst} shows no contribution to boson peak but a considerable heat capacity from electronic and lattice contribution, thus it can be subtracted from that of the glass to highlight the boson peak contribution. Fig. 2 (a) shows the boson peak of samples after single-step aging, it becomes more and more depressed as t_a increases, and the peak maximum shifts to higher T by ~2 K with t_a increasing from 0.1 to 102.4 min. Such aging effect on boson peak accords with previous observations in other BMGs [35-38]. Fig. 2 (b) shows the boson peak after double-step aging, remarkably, as t_a increases, it firstly becomes more and more pronounced and then depressed, showing a nonmonotonic evolution. For both single- and double-step aging, it is clear that with the higher strength of the boson peak, at the lower temperature occurs the peak maximum.

Figure 3 plots the t_a-dependent relative enthalpy change ΔH [Fig. 3(a)] and boson peak height [peak maximum of $(C_p\text{-}C_p^{\text{cryst}})/T^3$, Fig. 3(b)] for various aging protocols. During single-step aging, the ΔH [curve A in Fig. 3 (a)] and the boson peak height [curve I in Fig. 3 (b)] decrease monotonically until the metastable equilibrium state is attained after around 100 min, showing a typical aging effect. Nevertheless, as the glass was pre-aged at a lower temperature T_0, i.e., with additional thermal history

endowed, the structural relaxation behavior turns to exhibit a totally different manner [see curves B-F in Fig. 3(a)]. The t_a-dependent ΔH undergoes firstly an increase moving away from the equilibrium value till to a maximum followed by a decrease approaching it, showing a temporary neglect of the equilibrium state, thus, the memory effect is revealed. And the ΔH peak maximum occurs later as the pre-aging temperature T_0 or the pre-aging time t_0 increases. Fig. 3(b) also shows the surprising result that for double-step aging (curves II and III) the t_a-dependent boson peak height experiences an incipient increase to a maximum and a following decrease to merge with that of the single-step aging within the experimental sensitivity. For curve II, with T_0=648 K and t_0=20 min, the boson peak height value peaks at around t_a=1.6 min, in agreement with curve C in Fig. 3(a) under the same aging protocol. Likewise, the magnitude of boson peak [curve III in Fig. 3(b)] and relative enthalpy change ΔH [curve E in Fig. 3(a)] follow similar evolution and peak simultaneously at around t_a=3.2 min for the double-step aging of T_0=668 K and t_0=20 min. All in all, the boson peak, which reflects the anomaly in the frequency spectra of atomic vibration in amorphous materials, shows obvious history-dependent behaviors of memory effect and behaves akin to the structural relaxation manifested from enthalpy measurements.

In Fig. 4 the boson peak height vs.ΔH is plotted. Within the accuracy limit of the method of measuring the boson peak behavior, Fig. 4 shows that the boson peak intensity follows an almost linear relationship with the relative enthalpy change. The result allows a semi-quantitative construction of the correlation between the structural relaxation and boson peak behavior. The clear-cut experimental observation has been given that the boson peak behaves in line with the relative enthalpy change during not only single-step but also double-step isothermal aging, strongly indicating a close correlation between the slow structural relaxation and the fast boson peak dynamics in metallic glass. It is highly reminiscent of the observation by Grigera *et al*. [24] that the sampling of higher energy on the potential energy landscape leads to an increase in boson peak intensity. Structurally, the simulation by Shintani *et al*. [18] shows that large local (free) volume benefits local boson peak intensity over the Debye value. Recent works reveal that the boson peak intensity of severely deformed metallic

glasses can be strongly enhanced due to the formation of shear bands with excess free volume [35, 36]. Starting from this scenario, the appearance of memory effect during the double-step aging can be understood.

Phenomenological or semi-quantitative models have been employed to describe the relaxation dynamics with emphasis on the memory effect, for example, two-relaxation-time model [11], a combination of chemical and topological structural relaxation [12], and activation energy spectrum model [15]. These models for the understanding of memory effect are commonly based on the spatially randomly distributed local regions, within which the atomic motions can be detected and appear as secondary relaxations [39]. Due to the heterogeneous nature of glass, distinct local regions show enhanced or reduced mobility with respect to the average relaxation rate, resulting in a concomitant dispersion of relaxation times [5, 6, 9, 10]. Within the heterogeneous dynamics scenario, memory effect can be described in terms of the non-exponential relaxation function [2], but without giving a clear microscopic physical picture. The boson peak is also closely related to the soft localized regions [18-20]. Based on the activation energy spectrum model [15] the microscopic picture concerning the memory effect can be drawn. Flow units are any available and thermally (or mechanically) activated localized rearrangement [39, 40]. At the lower temperature T_0, the flow units with low activation energy come to be depleted (achieving metastable equilibrium). At the higher temperature T_a, the reactivation of these flow units takes place resulting in the observed increase in enthalpy and boson peak intensity. The flow units with high activation energy are still active at T_0, and at T_a further rearrangement continues resulting in the decrease of enthalpy and boson peak, and the reactivated flow units will subsequently return again to the metastable equilibrium, thus a nonmonotonic behavior was observed. The higher pre-aging temperature T_0 and/or pre-aging time t_0 results in the depletion of more flow units with high activation energy, and it takes more time for these flow units to be reactivated at T_a, so we observe the values of ΔH and boson peak intensity peak at longer t_a (see Fig.3).

Here arises a question of how a temperature rise brings about the reactivation of

the originally depleted flow units. A recent work by Ketov *et al*. [41] provides new insight that the thermal cycling of metallic glass to cryogenic temperatures cause atomic-scale structural rejuvenation. At low temperatures the effect of aging can be reduced and the temperature change will induce internal stresses that cause atomic scale non-affine deformation. Remarkably, the thermal cycling of partially relaxed BMGs can induce increased fraction of flow units and better plasticity than that of as-cast BMGs [41], suggesting that large as-cast heterogeneities (soft liquid-like regions) are prone to absorb a portion of the newly induced internal stresses. Structural relaxation has been proposed to be driven by atomic scale internal stress [7, 10], while as the thermal expansion coefficient of flow units varies from that of their neighbors, the originally depleted flow units are cast again into an incompatible stress environment as the temperature is elevated, resulting in additional internal stresses that bring back the BMG to higher energy state. Being the energy of inherent structure the relevant control parameter [24], an increase of boson peak intensity is observed.

Recent X-ray photo correlation spectroscopy studies on the aging of metallic glasses gives more atomic-scale details [42]. Following both dynamical and structural approaches, it pointed out that microscopic aging in fast-quenched metallic glasses can be ascribed to two processes: the first one which affects density until density inhomogeneities are completely released; the second one is an ordering on the medium range, which does not affect the density [42-44]. This scenario enables a clearer interpretation of our results. These two processes act together during the lower temperature fast aging step, which releases a good part of inhomogeneities by annihilation of flow units with lower activation barriers, and the glass attains microscopically a relatively homogeneous state [45]. As the glass is stepped quickly to higher temperatures, a mismatch of thermal expansion coefficient between neighboring local regions (medium range) induces new internal stresses that cause transient local disordering by atomic rearrangement (rejuvenation). While the second process of medium range ordering still goes on at the higher temperature step, the nonmonotonic behavior results. From this point of view, the memory effect is one corollary of the heterogeneous nature of glasses, and directly comes from a transient

local disordering accompanied by an enhancement in the boson peak intensity, which is an intrinsically universal feature of glasses and has been widely believed to originate from local soft regions [18-20].

In conclusion, through the memory effect, we bridge the structural relaxation and the universal boson peak feature in a typical Zr-based BMG. Consistent with enthalpy relaxation, boson peak shows memory effect. The observed contrasting monotonic versus nonmonotonic relaxation behavior of enthalpy and boson peak intensity in the single- and double-step aging, respectively, univocally indicates a close correlation between the slow structural relaxation and the fast boson peak dynamics. The results benefit the understanding of the history-dependent behaviors of memory effect and the anomalous low-energy excitation in glass.

Acknowledgements

We thank M. X. Pan, D. Q. Zhao, Z. Lu and W. C. Xiao for experimental assistance and discussions. This work was supported by the NSF of China (51271195) and MOST 973 Program (No. 2015CB856800).

References

[1] W. H. Wang, J. Appl. Phys. 99, 093506 (2006).

[2] I. M. Hodge, J. Non-Cryst. Solids 169, (1994).

[3] K. L. Ngai, *Relaxation and Diffusion in Complex Systems* (Springer, New York, 2011).

[4] L. Berthier, G. Biroli, Rev. Mod. Phys. 83, 587 (2011).

[5] J. C. Mauro, S. S. Uzun, and S. Sen, Phys. Rev. Lett. 102, 155506 (2009).

[6] R. Richert, Phys. Rev. Lett. 104, 085702 (2010).

[7] B. Ruta, *et al*., Phys. Rev. Lett. 109, 165701 (2012).

[8] C. Brun, *et al*., Phys. Rev. Lett. 109, 175702 (2012).

[9] M. Paluch, *et al*., Phys. Rev. Lett. 110, 015702 (2013).

[10] Z. Evenson, *et al*., Phys. Rev. Lett. 115, 175701 (2015).

[11] A. L. Greer and J. A. Leake, J. Non-Cryst. Solids 33, 291 (1979).

[12] A. van den Beukel, *et al*., Acta metall. 32, 1895 (1984).

[13] D. P. B. Aji, P. Wen, G. P. Johari, J. Non-Cryst. Solids 353, 3796 (2007).

[14] C. A. Volkert and F. Spaepen, Acta melall. 37, 1355 (1989).

[15] M. R. J. Gibbs, J. E. Evetts, J. A. Leake, J. Mater. Sci. 18, 278 (1983).

[16] B. Frick and D. Richter, Science 267, 1939 (1995).

[17] *Amorphous Solids: Low Temperature Properties*, edited by W. A. Phillips (Springer-Verlag, Berlin, 1981).

[18] H. Shintani and H. Tanaka, Nat. Mater. 7, 870 (2008).

[19] H. R. Schober, J. Non-Cryst. Solids 357, 501 (2011).

[20] B. B. Laird and H. R. Schober, Phys. Rev. Lett. 66, 636 (1991).

[21] V. G. Karpov, *et al*., Zh. Eksp. Teor. Fiz. 84, 760 (1983).

[22] U. Buchenau, *et al*., Phys. Rev. B 46, 2798 (1992).

[23] L. Gil, *et al*., Phys. Rev. Lett. 70, 182 (1993).

[24] T. S. Grigera, *et al*., Nature 422, 289 (2003).

[25] V. Lubchenko and P. G. Wolynes, Proc. Natl. Acad. Sci. U.S.A. 100, 1515 (2003).

[26] S. R. Elliott, Europhys. Lett. 19, 201 (1992).

[27] W. Schirmacher, *et al*., Phys. Rev. Lett. 98, 025501 (2007).

[28] H. R. Schober and C. Oligschleger, Phys. Rev. B 53, 11469 (1996).

[29] A. N. Vasiliev, *et al*., Phys. Rev. B 80, 172102 (2009).

[30] M. B. Tang, *et al*., Phys. Rev. B 72, 012202 (2005).

[31] S. N. Taraskin, *et al*., Phys. Rev. Lett. 86, 1255 (2001).

[32] A. I. Chumakov, *et al*., Phys. Rev. Lett. 106, 225501 (2011).

[33] F. H. Stillinger, Science 267, 1935 (1995).

[34] See Supplemental Material for experimental details and additional information.

[35] J. Bünz, *et al*., Phys. Rev. Lett. 112, 135501 (2014).

[36] Y. P. Mitrofanov, *et al*., Phys. Rev. Lett. 112, 135901 (2014).

[37] Y. Li, *et al*., J. Appl. Phys. 104, 013520 (2008).

[38] B. Huang, *et al*., J. Appl. Phys. 115, 153505 (2014).

[39] P. Luo, *et al*., Appl. Phys. Lett. 106, 031907 (2015); H. B. Yu, *et al*., National Sci. Rev. 1, 429 (2014).

[40] Z. Wang, B. A. Sun, H.Y. Bai and W.H. Wang, Nat. Commun. 5, 5823 (2014).

[41] S. V. Ketov, *et al*., Nature 524, 200 (2015).

[42] V. M. Giordano and B. Ruta, Nat. Commun 7, 10344 (2016).

[43] J. Bednarcik, *et al*., J. Alloys Comp. 504S, 155 (2010).

[44] M. Mao, *et al*., Phys. Rev. B 51, 2798 (1995).

[45] P. Luo, *et al*., Phys. Rev. B 93, 104204 (2016).

Figure captions

Figure 1. Enthalpy recovery after **(a)** single-step isothermal aging and **(b)** double-step isothermal aging for different aging time t_a, T_a=688 K for all cases. For the double-step aging T_0=648 K and t_0=20 min. The black solid lines represent the reference curve (Ref.) without isothermal aging. The inset in **(a)** is the relative enthalpy change ΔH against the t_a, the lines are the guide for the eyes, the solid red line for the single-step aging and the dash green line for the double-step aging.

Figure 2. Boson heat capacity peaks of samples from **(a)** single- and **(b)** double-step isothermal aging for different aging time t_a, T_a=688 K for all cases. For the double-step aging T_0=648 K and t_0=20 min.

Figure 3. (a) Relative enthalpy change ΔH against the aging time t_a for single-step (curve A) and double-step isothermal aging (curves B-F). For double-step aging, the pre-aging temperatures T_0 for cases B-E were 638 K, 648 K, 658 K and 668 K, respectively, the pre-aging time t_0=20 min. Case F with T_0=668 K and t_0=30 min. **(b)** Boson peak height against the t_a for single- (curve I) and double-step isothermal aging (T_0=648 K for curve II and T_0=668 K for curve III, t_0=20 min). T_a=688 K for all cases. The lines are drawn as a guide for the eyes.

Figure 4. Relationship between the boson peak height and the relative enthalpy change, the data from both single- and double-step aging are embraced. The dash line gives a guide for the eyes.

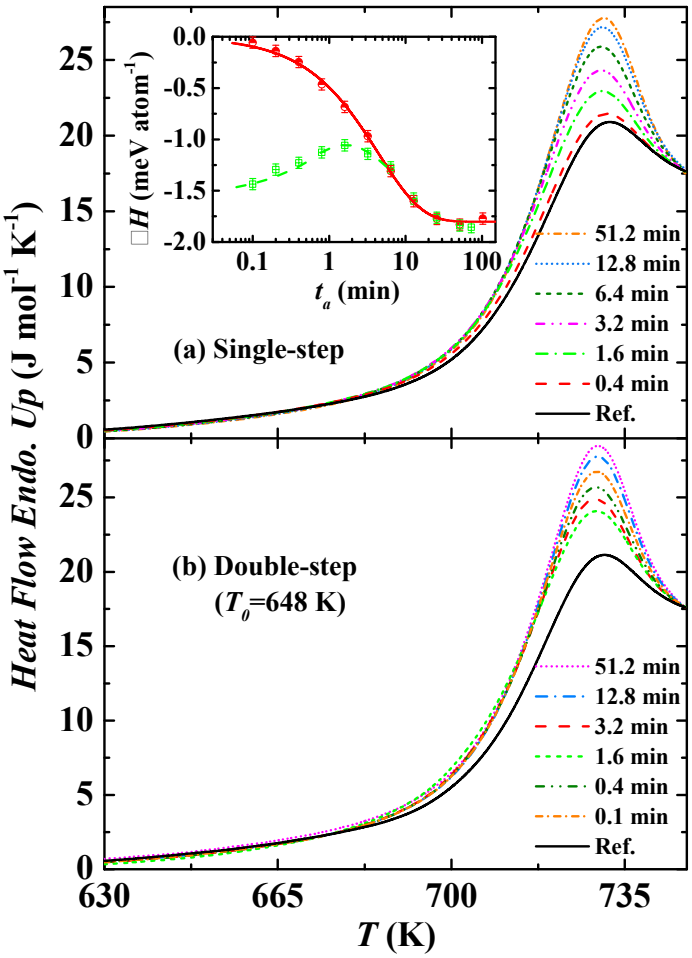

Fig. 1. Luo *et al.*

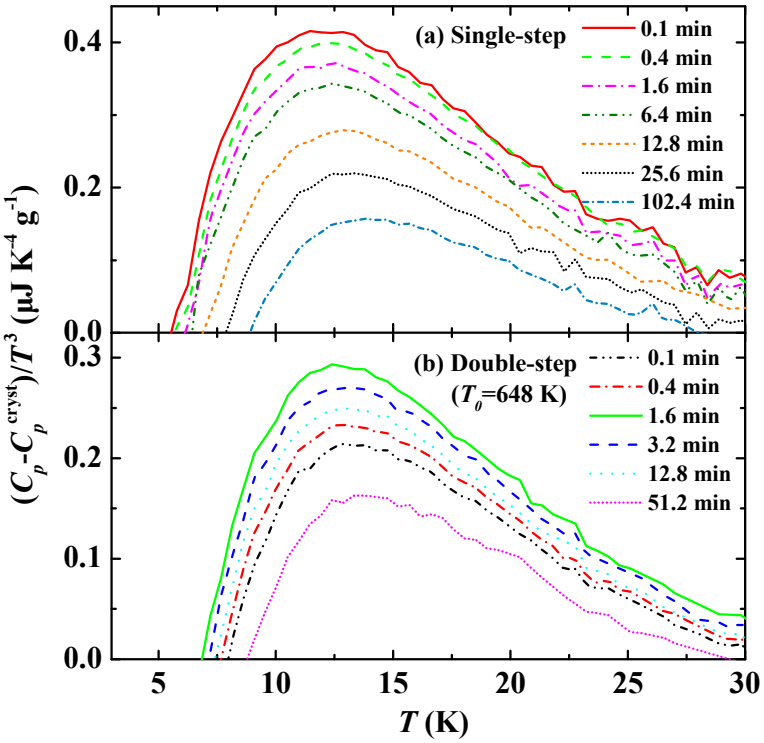

Fig. 2. Luo *et al.*

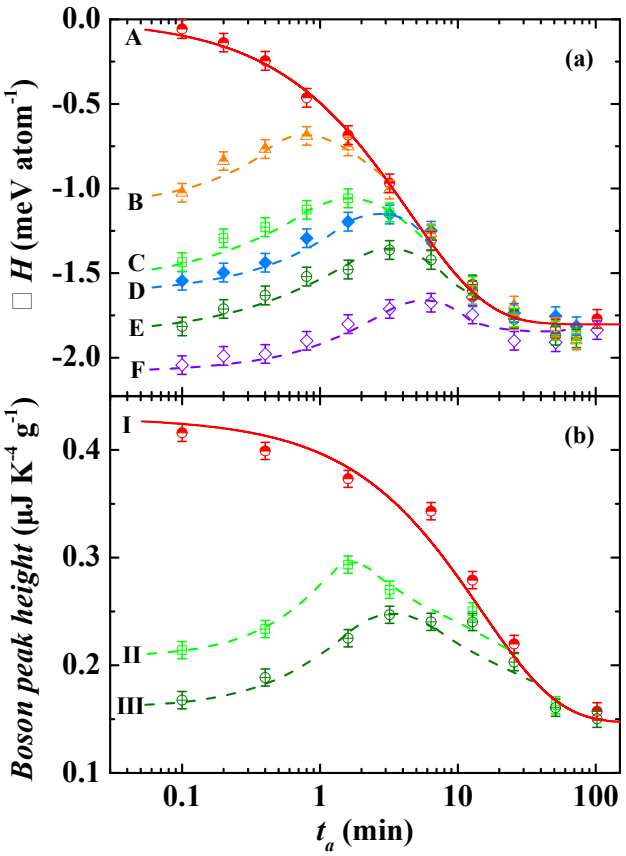

Fig. 3. Luo *et al.*

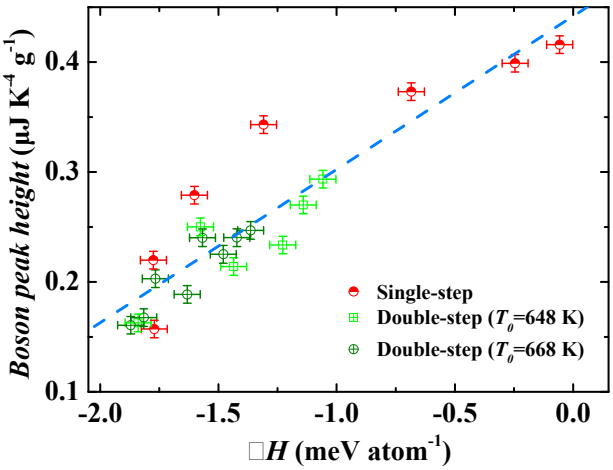

Fig. 4. Luo *et al.*